Microstructure, transport, and acoustic properties of open-cell foam samples: Experiments and three-dimensional numerical simulations [(*)]

Modélisation et Simulation Multi Echelle

MSME UMR 8208

→ Linking measured porosity and permeability to material micro-structure and resulting acoustic properties | [(*)] To appear in J. Appl. Phys 111 (2012) [DOI: 10.1063/1.3673523]

C. PERROT [(1,2,a)] – F. CHEVILLOTTE [(3)] – M. T. HOANG [(1,4)] – G. BONNET [(1)] – F.-X. BÉCOT [(3)]

L. GAUTRON [(5)] – A. DUVAL [(4)]

(1) Laboratoire de Modélisation et Simulation Multi Echelle (MSME) UMR CNRS 8208, Université de Paris-Est, 5 Bd Descartes, F-77454 Marne-la-Vallée cedex 2; **(2)** Université de Sherbrooke, Department of Mechanical Engineering, Québec J1K 2R1, Canada; **(3)** Matelys - Acoustique & Vibrations, 1 rue Baumer, F-69120 Vaulx-en-Velin; **(4)** Faurecia Acoustics and Soft Trim Division, R&D Center, Route de Villemontry, Z.I. BP13, F-08210 Mouzon; **(5)** Laboratoire Géomatériaux et Environnement LGE EA 4508, Université Paris-Est, 5 bd Descartes, F-77454 Marne-la-Vallée cedex 2. a) camille.perrot@univ-paris-est.fr

Introduction

The purpose of this paper is to present a technique based on first-principles calculations of transport parameters in reconstructed porous media which can be applied to model the acoustic properties of real foam samples predominantly open-cell (Fig. 1 & 2) and to compare its predictions to multi-scale experimental data (Figs. 2 & 5-6, and Tab. I).

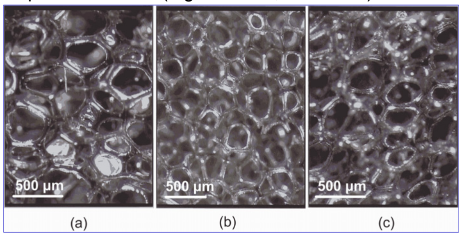

(a) (b) (c)

Fig 1. Typical micrographs of real foam samples: (a) R_1, (b) R_2, and (c) R_3. The average numbers n of edges per face for each photomicrograph are as follows: (a) R_1, $n_1 = 5.21 \pm 0.69$; (b) R_2, $n_2 = 4.94 \pm 0.56$; (c) R_3, $n_3 = 4.84 \pm 0.80$.

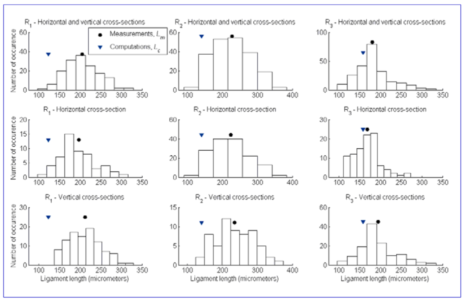

Fig 2. Ligament length distributions for real foam samples R_1 (left), R_2 (center), and R_3 (right). Labels (●) give the measured averaged ligament lengths obtained from micrographs, whereas labels (▾) indicate the computed ligament length Lc of the truncated octahedron unit-cell used for numerical simulations.

Foams	Method	ϕ (-)	Λ' (μm)	k_0 (m²)	α_0(-)	Λ (μm)	α_∞(-)	k_0' (m²)	α_0'
	Computations		506		1.22	297	1.02	5.01×10^{-9}	1.13
R_1	Measurements [a, b]	0.98		2.60×10^{-9}					
	Characterization [c, d]		440			129	1.12	8.30×10^{-9}	
	Computations		477		1.26	279	1.02	5.85×10^{-9}	1.14
R_2	Measurements [a, b]	0.97		2.98×10^{-9}					
	Characterization [c, d]		330			118	1.13	9.70×10^{-9}	
	Computations		647		1.22	373	1.01	8.18×10^{-9}	1.13
R_3	Measurements [a, b]	0.98		4.24×10^{-9}					
	Characterization [c, d]		594			226	1.06	13.10×10^{-9}	

Tab. I. Comparison between computed, measured, and characterized transport parameters of foam samples R_1, R_2, and R_3..

Hypothesis

Since the variability in the foam microstructures makes it very difficult to establish and apply local geometry models to study the acoustics of these foams, the use of a representative periodic cell (Fig. 3) is proposed to quantitatively grasp the complex internal structure of predominantly open-cell foam samples.

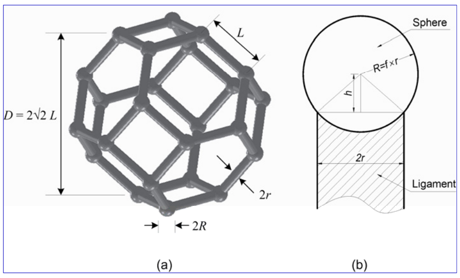

Fig 3. Basic 3D periodic foam model geometry: (a) a regular truncated octahedron with ligaments of circular cross-section shape (length L, radius r), and (b) spherical nodes (radius R) at their intersections. Note that f is a spherical node size parameter which is set to 1.5.

Analytical expressions of porosity **Φ**, and generalized hydraulic radius **Λ'** (or specific surface area S_p) :

$$\Phi = 1 - \left(\frac{3\sqrt{2}\pi}{16}\right)\left(\frac{2r}{L}\right)^2 - \left(\frac{\sqrt{2}\pi D_1}{16}\right)\left(\frac{2r}{L}\right)^3 \qquad \Lambda' = 2\Phi / Sp$$

$$D_1 = -f^3 + 2(f^2 - 1)\sqrt{f^2 - 1} \qquad R = f \times r \qquad f \geq \sqrt{2}$$

$$\Lambda' = \left[\frac{16\sqrt{2} / \left(\frac{2r}{L}\right)^3 - 6\pi / \left(\frac{2r}{L}\right) - 2\pi D_1}{3\pi\left(2 / \frac{2r}{L} + D_2\right)}\right] \times r$$

$$D_2 = -f^2 + 2(f - 1)\sqrt{f^2 - 1}$$

These expressions are linking **micro-** to **macro-**geometric parameters.

Method

Implications of the pore size dispersion:
The permeability is not governed by an average cell, but by a critical one, scaled as follows

- Step 1: Porosity measurement → $2r/L$ (non-dimensional cell)
- Step 2: Permeability measurement k_0
- Step 3: Permeability computation on the non-dimensional cell k_{nd} (Stokes equations)
- Step 4: Finding out the critical dimension, D.

$$k_0 = D^2 k_{nd}$$

Transport parameters are then computed by solving the steady Stokes, electric conduction, and diffusion controlled reaction equations in the critical unit-cell (Fig. 4).

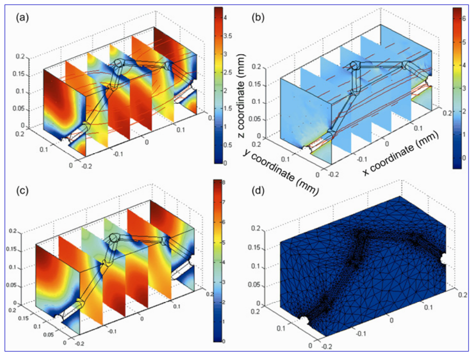

Fig 4. (Color online) Asymptotic fields for 1/4th of the reconstructed foam sample period R_1: (a) low-frequency scaled velocity field [$\times 10^{-9}$ m2], (b) high-frequency scaled velocity field [-] for an external unit field , (c) low-frequency scaled temperature field [$\times 10^{-9}$ m²], and (d) corresponding mesh domain with 41 372 lagrangian P_2P_1 tetrahedral elements.

The frequency-dependent visco-inertial and thermal response functions are then derived from approximate but robust analytical models accounting for the causality principle and therefore for the Kramers-Kronig relations (Fig. 5).

Results Summary

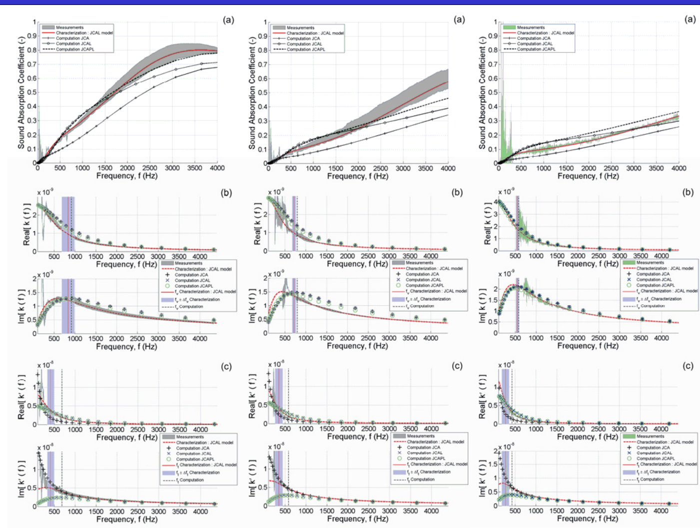

Fig 5. (a) Normal incidence sound absorption coefficient, dynamic viscous permeability, and (c) dynamic thermal permeability. Comparison between measurements, characterization, and computations (this work). Foam sample R_1 (Left), R_2 (Center), and R_3 (Right). Sample thicknesses: 25 mm, 15 mm, and 15 mm, respectively.

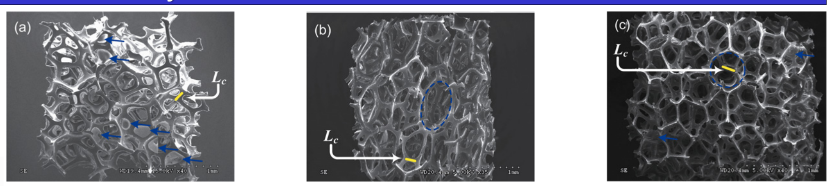

Fig 6. Typical scanning electron microscope images of real foam samples. (a) R_1, showing a relatively great number of membranes (indicated by arrows) compared to R_2 and R_3 foams. (b) R_2, having a degree of anisotropy equal to 1.75 as illustrated with a superimposed ellipse. (c) R_3, exhibits only few isolated residual membranes (thermal reticulation process), with rather spherical pore shapes (schematically represented by a circle). For each real foam sample, a line corresponding to the specific length *Lc* clearly shows the typical size of an opening which could participate to a **critical path**.

Concluding Remarks

A three-dimensional idealized periodic unit-cell (PUC) based method to obtain the acoustic properties of three predominantly open-cell foam samples was described. The first step was to provide the local characteristic lengths of the representative unit cell. For isotropic open cell foams, two input parameters were required, the porosity and the static viscous (hydraulic) permeability. Long-wavelengths acoustic properties were derived from the three-dimensional reconstructed PUC by solving the boundary value problems governing the micro-scale propagation and visco-thermal dissipation phenomena with adequate periodic boundary conditions, and further field phase averaging. The computed acoustic properties of the foams were found to be in relatively good agreement with standing wave tube measurements. A close examination of the real foam sample ligament length distribution as observed from micrographs, and its comparison with the characteristic size of the local geometry model, showed evidences of membrane and cellular anisotropy effects discussed by means of critical path considerations.

3rd Symposium on the Acoustics of Poro-Elastic Materials (SAPEM 2011), December 14-15-16, 2011 Ferrara (Italy)
Acoustic Porous Media: Integration Across Scales